

INTERFEROMETRIC CO OBSERVATIONS OF SUBMILLIMETER-FAINT, RADIO-SELECTED STARBURST GALAXIES AT $z \sim 2$

S. C. CHAPMAN,^{1,2} R. NERI,³ F. BERTOLDI,⁴ IAN SMAIL,⁵ T. R. GREVE,⁶ D. TRETHEWEY,¹ A. W. BLAIN,⁷
P. COX,³ R. GENZEL,⁸ R. J. IVISON,^{9,10} A. KOVACS,⁴ A. OMONT¹¹ AND A. M. SWINBANK⁵

Draft version October 30, 2018

ABSTRACT

High-redshift, dust-obscured galaxies – selected to be luminous in the radio but relatively faint at $850\,\mu\text{m}$ – appear to represent a different population from the ultra-luminous submillimeter- (submm-) bright population. They may be star-forming galaxies with hotter dust temperatures or they may have lower far-infrared luminosities and larger contributions from obscured active galactic nuclei (AGN). Here we present observations of three $z \sim 2$ examples of this population, which we term *submm-faint radio galaxies* – SFRGs in CO(3–2) using the IRAM Plateau de Bure Interferometer to study their gas and dynamical properties. We estimate the molecular gas mass in each of the three SFRGs ($8.3 \times 10^9 M_\odot$, $< 5.6 \times 10^9 M_\odot$ and $15.4 \times 10^9 M_\odot$, respectively) and, in the case of RG J163655, a dynamical mass by measurement of the width of the CO(3–2) line ($8 \times 10^{10} \text{ csc}^2 i M_\odot$). While these gas masses are substantial, on average they are $4\times$ lower than submm-selected galaxies (SMGs). Radio-inferred star formation rates ($< \text{SFR}_{\text{radio}} > = 970 M_\odot \text{ yr}^{-1}$) suggest much higher star-formation efficiencies than are found for SMGs, and shorter gas depletion time scales ($\sim 11 \text{ Myr}$), much shorter than the time required to form their current stellar masses ($\sim 160 \text{ Myr}$; $\sim 10^{11} M_\odot$). By contrast, SFRs may be overestimated by factors of a few, bringing the efficiencies in line with those typically measured for other ultraluminous star-forming galaxies and suggesting SFRGs are more like ultraviolet- (UV-) selected star-forming galaxies with enhanced radio emission. A tentative detection of RG J163655 at $350\,\mu\text{m}$ suggests hotter dust temperatures – and thus similar gas-to-dust mass fractions – as the SMGs. We conclude that SFRGs’ radio luminosities are larger than would naturally scale from local ULIRGs given their gas masses or gas fractions.

Subject headings: galaxies: evolution — galaxies: formation — cosmology: observations — galaxies: starbursts — galaxies: high-redshift

1. INTRODUCTION

Submm surveys have provided an efficient probe of star-formation activity in ultraluminous infrared (IR) galaxies (ULIRGs, $> 10^{12} L_\odot$) in the distant Universe (e.g., Smail, Ivison & Blain 1997; Hughes et al. 1998; Barger et al. 1998), with bright submm emission providing unambiguous evidence of massive quantities of dust, heated predominantly by young stars rather than AGN (e.g., Chapman et al. 2003a; Alexander et al. 2005; Menendez-Delmestre et al. 2007; Valiante et al. 2007; Pope et al. 2008). Before the availability of the Atacama Large Millimeter Array (ALMA), confusion will continue to limit the sensitivity of current submm sur-

veys. As a result, many ULIRGs fall below the detection limits due to variations in their spectral energy distributions (SEDs) – usually parameterized in terms of dust temperature (T_d) – meaning that entire populations of star-forming galaxies may have been missed by submm surveys.

For a fixed far-infrared luminosity (FIR), a galaxy with a higher T_d will be weaker in the submm at $850\,\mu\text{m}$ than a galaxy with a lower T_d . Specifically, raising T_d from the canonical $\sim 35 \text{ K}$ for SMGs to 45 K will result in a factor $\sim 10\times$ drop in $850\,\mu\text{m}$ flux density (Blain 1999; Chapman et al. 2004). These galaxies should, though, be accessible in the radio waveband, regardless of their specific SEDs, since the radio correlates with the integrated FIR emission (Helou et al. 1985) with a small $\sim 0.2\text{dex}$ dispersion and no observable dependence on SED type. However, there is potential for large AGN contaminations in the radio, as has often been the case with mid-IR selection of $z > 1$ ULIRGs (e.g., Houck et al. 2005; Yan et al. 2005, 2007; Sajina et al. 2007; Weedman et al. 2006a, 2006b; Desai et al. 2006) and the facilities required to provide the high-resolution, multi-frequency radio data needed to decontaminate the samples (e.g., Ivison et al. 2007a) are not yet available.

Substantial populations of apparently star-forming galaxies at $z \sim 2$ have been uncovered through deep 1.4-GHz radio continuum observations, many of which are not detected at submm wavelengths with the current generation of instruments (Barger et al. 2000; Chapman et al. 2001, 2003b, 2004a – hereafter C04). These galax-

¹ Institute of Astronomy, Madingley Road, Cambridge, CB3 0HA, UK.

² University of Victoria, Victoria, BC, V8W 3P6, Canada.

³ Institut de Radio Astronomie Millimétrique (IRAM), St Martin d’Hères, France.

⁴ Argelander Institut für Astronomie, Universität Bonn, Auf dem Hugel 71, 53121 Bonn

⁵ Institute for Computational Cosmology, Durham University, South Road, Durham DH1 3LE, UK.

⁶ Astronomy Department, Max-Planck Institut für Astronomie, Königstuhl-17, D-69117, Heidelberg, Germany

⁷ California Institute of Technology, Pasadena, CA 91125.

⁸ Max-Planck Institut für extraterrestrische Physik (MPE), Garching, Germany.

⁹ UK Astronomy Technology Centre, Royal Observatory, Blackford Hill, Edinburgh EH9 3HJ, UK.

¹⁰ Institute for Astronomy, University of Edinburgh, Royal Observatory, Blackford Hill, Edinburgh EH9 3HJ, UK.

¹¹ Institut d’Astrophysique de Paris, CNRS, Université de Paris, Paris, France.

ies are luminous in the radio and spectroscopy suggests that star formation is powering their bolometric output (there is little or no sign of high-ionization emission lines, characteristic of AGN in their UV/optical spectra). These galaxies could, in principle, span a range in properties from deeply obscured AGN to far-IR-luminous starbursts. In the latter case, one would expect a different SED from a typical SMG – a higher T_d for instance. These *submm-faint radio sources* have a large volume density at $z \sim 2$, even larger than the SMGs (Haarsma et al. 1998; Richards et al. 1999; Chapman et al. 2003a, C04; Barger et al. 2007). There are $\rho = 2 \times 10^{-5} \text{ Mpc}^{-3}$ radio sources with $L_{1.4\text{GHz}} > 10^{31} \text{ erg s}^{-1} \text{ Hz}^{-1}$ at $z \sim 2$ compared with $\rho = (6.2 \pm 2.3) \times 10^{-6} \text{ Mpc}^{-3}$ for SMGs brighter than 5 mJy at 850 μm at the same epoch (Chapman et al. 2003b, 2005). As essentially all of these SMGs form a subset of these radio sources (Chapman et al. 2005; Pope et al. 2006; cf. Ivison et al. 2002) this implies $\sim 14 \times 10^{-6} \text{ Mpc}^{-3}$ luminous radio sources remain undetected at submm wavelengths. Understanding the exact properties of these galaxies is therefore of great importance. If they are all forming stars at the rates implied by their radio luminosities, they would triple the observed SFR density (SFRD) at $z \sim 2$. By contrast, if their radio luminosity comes from a mix of star formation and AGN, they have less impact on the global SFRD but they increase the highly obscured AGN fraction at these epochs (e.g., Daddi et al. 2007a; Casey et al. 2008) and contribute substantially to black hole growth.

Together with other observations, the redshifted cooling emission lines of CO allow us to assess and compare the energy source of SFRGs with that of SMGs and other distant star-forming galaxies via measurements of their gas and dynamical masses. In this paper, we present the results of a pilot study with the IRAM – Plateau de Bure Interferometer to detect molecular gas in SFRGs through the rotational CO(3–2) line emission. In § 2 we describe the sample properties and observations both with PdBI and other facilities. Section § 3 presents the CO(3–2) detections and limits obtained from the PdBI observations, § 4.1 estimates gas properties, star-formation rates and efficiencies, and § 4.2 compares the SFRGs to other galaxy populations. Finally § 5 discusses the results and places them in a broader galaxy evolution context. Throughout we assume a cosmology with $h = 0.7, \Omega_\Lambda = 0.72, \Omega_M = 0.28$ (e.g., Hinshaw et al. 2008).

2. SAMPLE PROPERTIES AND OBSERVATIONS

Our sample is drawn from an expansion of the C04 submm-faint, radio-selected galaxy (SFRG) program, with galaxies drawn from several deep radio survey fields with typical sensitivity limits of $\sigma = 4\text{--}8 \mu\text{Jy}$ (e.g., Biggs & Ivison 2006). In the submm, the survey fields are imaged to a typical depth of $\sigma_{850\mu\text{m}} \sim 1\text{--}2 \text{ mJy}$ (e.g., Scott et al. 2002, Borys et al. 2003). We selected sources with redshifts, radio luminosities, and submm limits typical of the population ($\langle z \rangle = 2.1, \langle L_{1.4\text{GHz}} \rangle = 2 \times 10^{31} \text{ erg s}^{-1} \text{ Hz}^{-1}, L_{850\mu\text{m}} < 1 \times 10^{31} \text{ erg s}^{-1} \text{ Hz}^{-1}$ ($< 2 \text{ mJy}$ for $z \sim 2$) at the $\sim 2\sigma$ level, lying within $\pm 1\sigma$ of the median SFRG in (C04), and observing RG J163655 and RG J131236 based on suitability of RA and confidence in the optical spectroscopic redshifts. A third source from our sample, RG J123711, was observed pre-

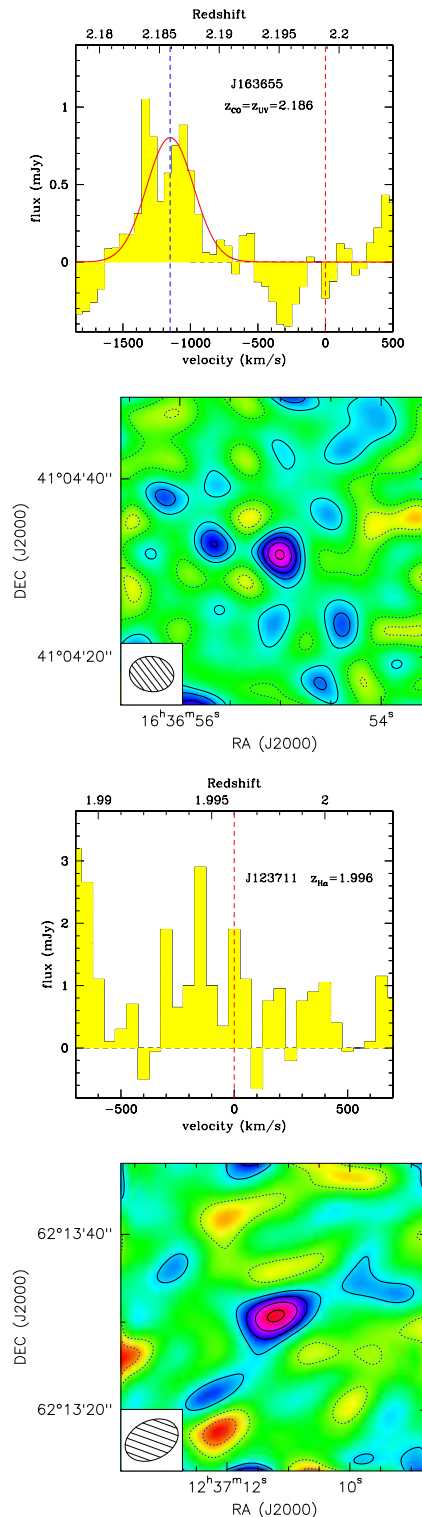


FIG. 1.— **top panels:** CO(3–2) spectra for the two candidate detections. The spectra are shown smoothed with a 50 km/s boxcar filter, and with respect to the zero velocity offsets defined from the H α emission line redshift (red dashed line). The best-fit Gaussian profile is shown for the emission line in RG J163655, along with the Uv-Inferred redshift from inter-stellar absorption lines (blue dashed line). **bottom panels:** velocity-averaged spatial maps of CO emission, from -1500 to -800 km s^{-1} (RG J163655) where contours are from -1 to 5σ in steps of σ ($0.05 \text{ mJy beam}^{-1}$). RG J123711 does not represent a formal CO detection. We measure a significance of 3.2σ integrating over the full band). The field of view, on a side, is $35''$, with the size of the beam shown to the lower left. Both CO emitters lie exactly at the radio source position to within $1''$.

viously with PdBI in the same field as an SMG in the program described by Neri et al. (2003) and Greve et al. (2005), and we include this object here. We note that while the neighboring SMG (SMM J123712.0+621326) lies only $8''$ to the south-east, we are confident that RG J123711 is not a luminous submm emitter. Firstly, SMM J123712, has a strong CO line detection (Smail et al., in preparation) with a $\sim 5\sigma$ detection $S_{\text{CO}(3-2)} = 1.2 \text{ Jy km s}^{-1}$, comparable to typical SMGs from Greve et al. (2005). Secondly, the $850\text{-}\mu\text{m}$ emission peak (with a $R=7''$ beam) in our SCUBA map is centered on the radio source position, whereas no significant peak is observed at the position of RG J123711. Removing a $850\text{-}\mu\text{m}$ point source from the position of SMM J123712 reveals an even lower $850\text{-}\mu\text{m}$ flux density ($0.1 \pm 1.2 \text{ mJy}$) at the position of RG J123711 than the $2.2 \pm 1.2 \text{ mJy}$ conservatively adopted for our calculations (Table 2). Importantly, the small $850\text{-}\mu\text{m}/1.4\text{-GHz}$ flux ratio for this source is clearly comparable to SFRGs and not to the typical radio-detected SMGs in Chapman et al. (2005) or Ivison et al. (2007b). The properties of these SFRGs are listed in Tables 1 and 2, and displayed in Figs 1 and 2.

2.1. PdBI observations

RG J163655 and RG J131236 were observed in their redshifted CO(3–2) lines and in the continuum at $\sim 108 \text{ GHz}$ using the newly refurbished PdBI receivers for 11.5 and 4.8 hr, respectively. Observations were made in D configuration on 2007 January 24, April 28, May 08 and June 03, with good atmospheric phase stability (seeing, $0.7\text{--}1.4''$) and reasonable transparency (0.5 mm of precipitable water vapor). For RG J163655, the $\text{H}\alpha$ redshift showed a considerable offset from that inferred from UV absorption and emission lines. While this was conceivably due to a large velocity starburst wind ($\sim 1300 \text{ km s}^{-1}$), we considered the possibility that one redshift might have calibration or resolution problems. We therefore observed RG J163655 split over two slightly offset frequency settings to span all measured redshifts. The overall flux scale for each observing epoch was calibrated using a variety of sources. In each observing epoch between three and six sources were used. The visibilities were resampled to a velocity resolution of 55 km s^{-1} (20 MHz) providing 1σ line sensitivities of $1.6 \text{ mJy beam}^{-1}$. The corresponding synthesized beam, adopting natural weighting, was similar for both sources, $5.0''$ by $4.0''$ at PA ~ 80 degrees, east of north. Observations of RG J123711 proceeded similarly to those described by Greve et al. (2005). The PdBI data for all three SFRGs were calibrated, mapped and analyzed using the GILDAS software package. The CO(3–2) spectra and images of the two candidate SFRG detections, RG J163655 and RG J123711, are shown in Fig. 1.

2.2. Other Observations

Spitzer observations of the SFRGs in this paper were taken with the Infrared Array Camera (IRAC) and the Multi-band Imaging Photometer (MIPS) through various GTO and Legacy programs.

RG J163655: In addition to the SCUBA $850\text{-}\mu\text{m}$ photometry, observations were obtained at $350\text{-}\mu\text{m}$ with the SHARC2 camera (Dowell et al. 2005) on the Caltech Submillimeter Observatory as part of the imaging campaign

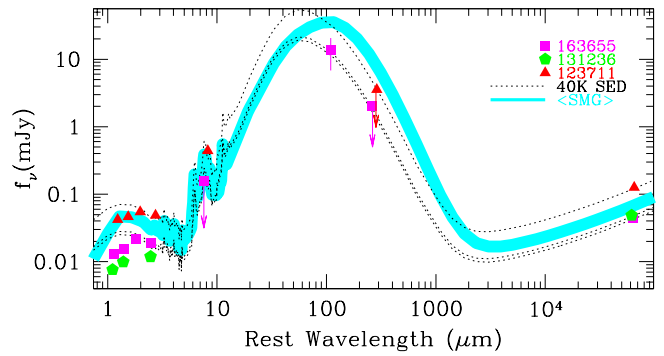


FIG. 2.— SEDs for RG J163655, RG J131236 and RG J123711. A local galaxy SED with $T_d = 40 \text{ K}$ (from Dale et al. 2003) is shown, normalized to the radio point in each case. An average fit to the SEDs of representative SMGs is shown as a heavy line (Chapman et al. 2005; Kovacs et al. 2006; Hainline et al. 2008).

of Kovacs et al. (2006), where observational details can be found. A near-IR spectrum from UKIRT/UIST covering the $\text{H}\alpha/[\text{N II}]$ region (Swinbank et al. 2006) finds a large $\text{H}\alpha/[\text{N II}]$ ratio suggestive of a relatively low metallicity, $[\text{Fe}/\text{H}] \sim -0.9$, and no strong AGN component. While the $[\text{O III}]\lambda 500.7$ region was also covered with the instrument, we did not clearly detect any emission lines, setting a limit on the $[\text{O III}]\lambda 500.7$ line of $3.75 \times 10^{-17} \text{ W m}^{-2}$ again suggesting that an AGN does not dominate the energetics of this galaxy. The line width of the $\text{H}\alpha$ emission ($\text{FWHM}_{\text{rest}}$) is $420 \pm 100 \text{ km s}^{-1}$ and the integrated line flux of $5.0 \times 10^{-19} \text{ W m}^{-2}$ then suggests a SFR uncorrected for dust extinction of $150 \pm 50 \text{ M}_{\odot} \text{ yr}^{-1}$ (Kennicutt 1998). The 1.4-GHz radio emission was unresolved by the Very Large Array (VLA) in its A configuration (Biggs & Ivison 2006). A relatively compact UV morphology is observed in the *Hubble Space Telescope* imaging, with $R_{1/2} = 0.25''$ (Swinbank et al. 2006).

RG J131236: In C04, the optical (rest-frame UV) spectrum was presented, showing $\text{Ly}\alpha$ in emission but all other detectable lines in absorption, and was classified as a pure starburst. The near-IR spectrum of RG J131236 from Keck/NIRSPEC covering the $\text{H}\alpha/[\text{N II}]$ region (Swinbank et al. 2004), again finds a large $\text{H}\alpha/[\text{N II}]$ ratio suggestive of a low metallicity, $[\text{Fe}/\text{H}] \sim -0.9$. The line width of the $\text{H}\alpha$ emission is $450 \pm 220 \text{ km s}^{-1}$ and the integrated line flux of $2.3 \pm 1.2 \times 10^{-19} \text{ W m}^{-2}$ then suggests an SFR uncorrected for dust extinction of $110 \pm 40 \text{ M}_{\odot} \text{ yr}^{-1}$. The radio emission was unresolved by the VLA. Only ground-based imaging exists for this SFRG, showing a faint, unresolved source in $0.8''$ seeing.

RG J123711: An X-ray-detection and obscured AGN classification due to its X-ray luminosity by Alexander et al. (2005) contrasts a PAH-dominated mid-IR spectrum obtained by Pope et al. (2008), showing no obvious AGN component. No rest-frame UV spectrum for RG J123711 has been published as there are no detected features. The redshift is based entirely on the near-IR spectrum where RG J123711 was detected with Keck/NIRSPEC (Swinbank et al. 2004), once again finding a large $\text{H}\alpha/[\text{N II}]$ ratio suggestive of an $[\text{Fe}/\text{H}] \sim -0.8$. The narrow line width of the $\text{H}\alpha$ emission ($112 \pm 45 \text{ km s}^{-1}$) and the integrated line flux of $0.4 \pm 0.3 \times 10^{-19} \text{ W m}^{-2}$ suggests an

SFR uncorrected for dust extinction of $16 \pm 9 \text{ M}_\odot \text{ yr}^{-1}$. Radio imaging of this SFRG with MERLIN ($0.3''$ synthesized beam; Casey et al. 2008b) reveals a double source structure with a $\sim 1''$ elongated feature and a relatively compact $R_{1/2}=0.4''$ component.

3. RESULTS

The velocity-integrated line fluxes or limits for all three SFRGs are listed in Table 1. For RG J163655, inspection of the data cube shows a significant 4.9σ detection of CO(3–2) line emission at the phase center, integrated over the velocity channels at $\sim -1000 \text{ km s}^{-1}$ with a velocity width of 400 km s^{-1} FWHM. Fitting a Gaussian profile to the CO spectrum, we derive a best-fit redshift for the CO(3–2) emission of $z = 2.1859 \pm 0.0002$, and estimate the CO flux is by summing the channels from -2σ to $+2\sigma$ of Gaussian fit to the line. We note that no significant continuum emission is detected from the line-free region ($\sim 650 \text{ MHz}$ of bandwidth) down to a 1σ sensitivity of $0.07 \text{ mJy beam}^{-1}$, consistent with the submm limit, assuming a dust spectral index, $\nu^{+3.5}$, for a modified blackbody with emissivity, $\beta = +1.5$. For RG J131236 no significant emission is observed at the phase center, although the limit on the CO gas mass is still of great interest relative to the SMGs. For RG J123711 we tentatively detected (3.2σ) a positive signal integrated over the full band from -600 to $+600 \text{ km s}^{-1}$, centered on the H α determined redshift of $z = 1.996$. A precise CO redshift cannot be determined for RG J123711 as the line shape cannot be determined in the low S/N spectrum. To assess the possibility that we have simply detected continuum in this source, we analyze the radio spectral index, measured to be steep from the $8.4 \text{ GHz}/1.4 \text{ GHz}$ flux ratio (Muxlow et al. 2005), $S_\nu \propto \nu^{-0.69}$, and the synchrotron contribution at $\sim 3 \text{ mm}$ is negligible. This does not however preclude a contribution from an AGN component with the opposite spectral slope emerging at higher frequencies. It is clear that the full radio spectrum is needed to explore this issue, as well as the possibility of an obscured AGN.

In RG J163655, the CO-inferred redshift is close to the redshift measured from various interstellar absorption lines in the Keck/LRIS UV spectrum, but is blue shifted by 1100 km s^{-1} from the H α line detected by Swinbank et al. (2006). Re-analysis of the near-IR spectrum does not significantly change the result as the sky line calibrations appear to be as presented in Swinbank et al. (2006). If the detected line were dominated by [N II] with $\text{H}\alpha/[\text{N II}] < 1$ – and we stress that there is no evidence in the spectrum of this – then the implied velocity offset would be $\sim 800 \text{ km s}^{-1}$, somewhat closer to the average CO velocity and consistent with the higher velocity peak in the detected CO profile. We cannot attribute the CO emission to an offset companion (as was the case for SMG J09431 in Tacconi et al. 2006) as the CO centroid is exactly at the near-IR and radio position to within the $1''$ centroiding uncertainty ($\sim \text{beam size} \times (\text{S/N})^{-1}$). The H α -inferred redshift has not always been representative of the CO redshift in SMG surveys (the average CO–H α offset is 150 km s^{-1}), presumably because the luminous core is so deeply dust enshrouded that wind outflows or satellite H II regions are more strongly detected in H α . We therefore put forward the hypothesis that we are detecting a highly dust-obscured gas-rich galaxy in

CO(3–2), either a companion seen in projection or else one not well sampled by the H α observations. The rest-frame FWHM of the CO line is $376 \pm 40 \text{ km s}^{-1}$, close to that found in H α by Swinbank et al. (2006), but likely a coincidence given that the CO and H α redshifts are discrepant.

The $350 \mu\text{m}$ SHARC-2 imaging of RG J163655 shows a tentative continuum detection, $S_{350 \mu\text{m}} = 2.4 \pm 6.5 \text{ mJy}$ at the radio position, however given the telescope pointing errors and the low signal-to-noise (S/N) of any expected emission, we search a region comparable to the beam size ($9''$). A 2σ peak ($S_{350 \mu\text{m}} = 13.7 \pm 6.9 \text{ mJy}$) lies $7''$ from the radio position at $16^{\text{h}} 36^{\text{m}} 54.6^{\text{s}}, +41^\circ 04' 28'' \text{ J2000}$. Within this area there are only ~ 3 SHARC-2 beams and the chance of a spurious 2σ peak is only $\sim 6\%$. There is a high likelihood ($\sim 90\%$) that this peak is related to RG J163655 and this flux range is completely consistent with our SED fit to the radio photometry for RG J163655 (Fig. 2).

We calculate from the integrated CO(3–2) intensity (Jy km s^{-1}) the line luminosities and estimate the total cold gas masses ($\text{H}_2 + \text{He}$) (listed in Table 1). We adopt $L'_{\text{CO}(3-2)} = 3.25 \times 10^7 S_{\text{CO}(3-2)} \nu_{\text{obs}}^{-2} (1+z)^{-3} D_L^2$, consistent with Solomon & Vanden Bout (2005).

We assume both a line luminosity ratio of $r_{32} = \frac{L'_{\text{CO}(3-2)}}{L'_{\text{CO}(1-0)}} = 1$ (i.e. a constant brightness temperature) and a CO-to- H_2 conversion factor of $\alpha = 0.8 \text{ M}_\odot \text{ K km s}^{-1} \text{ pc}^2$. These values are appropriate for local galaxy populations exhibiting similar levels of star-formation activity to our SFRGs (e.g., local ULIRGs – Solomon et al. 1997), and this choice also facilitates comparison with SMGs modeled with the same values (Greve et al. 2005). We discuss later how the affect of adopting typical Milky Way values α_{CO} and r_{32} .

All three SFRGs show a peaked SED in the mid-IR (Fig. 2) suggesting that this spectral region is dominated by stars rather than AGN. These properties are used to derive the rest-frame K -band ($\sim 2.2 \mu\text{m}$) flux, and convert to a stellar mass, in a manner similar to Borys et al. (2005), adopting their $L_K/\text{M}_\odot = 3.2$ characteristic of a burst with an age of $\sim 250 \text{ Myr}$. We interpolated between IRAC bands to estimate $S_{2.2 \mu\text{m}}$ (Table 3).

3.1. Derived Properties

We then proceed to estimate various derived properties (listed in Table 3). Starting with the gas surface density, for RG J123711, we assume the CO emission traces the same large, extended morphology ($> 1''$ FWHM diameter) traced by resolved MERLIN radio imaging (see Casey et al. 2008b for details), suggesting a low gas surface density. For RG J163655 and RG J131236, neither the CO emission nor the VLA radio emission is resolved. Without further information beyond the optical imaging described previously, we assume the gas in these two SFRGs is distributed in a disk with a similar radius to SMGs (e.g., Tacconi et al. 2008) of $R_{1/2}=1.7 \text{ kpc}$ ($0.25''$), resulting in higher inferred gas surface densities. The CO luminosities for the three SFRGs are plotted as a function of FIR luminosity and compared to other high-redshift galaxies detected in CO in Fig. 3.

A dynamical mass for the well-detected RG J163655 can be estimated by analyzing the CO line profile. We

base our analysis on a single Gaussian fit to the line. CO emission is comparatively immune to the effects of obscuration and outflows and therefore provides a unbiased measurement of dynamics within the CO-emitting region. The line width of the CO emission ($410 \pm 40 \text{ km s}^{-1}$) implies a dynamical mass of $(8.4 \pm 2.1) \times 10^{10} \text{ csc}^2 i \text{ M}_\odot$, assuming the gas lies in a disk with inclination i and a radius of $0.25''$ (1.7 kpc). Based on this, we calculate a gas to dynamical mass fraction of $f = \frac{M_{\text{gas}}}{M_{\text{dyn}}} \sim 0.10 \sin^2 i$. We note that the mean angle of randomly oriented disks with respect to the sky plane in three dimensions is $i = 30^\circ$ (Carilli & Wang 2006), resulting in an average inclination correction of $\text{csc}^2 i = 4$.

4. ANALYSIS

4.1. Star-Formation Rate and Efficiency

The radio luminosity of the SFRGs forms our baseline estimate for the far-IR luminosity and SFRs (listed in Table 3), since we have only upper limits at 450 and $850 \mu\text{m}$. We caution however that our flux-limited radio selection biases our sample to find objects of the same radio luminosity as SMGs, regardless of the origin of the radio power. There are clear examples within the wider SFRG sample where AGN dominate the radio power despite an apparent starburst spectrum in the rest-frame UV (e.g., Casey et al. 2008a). The average $\langle \text{SFR}_{\text{radio}} \rangle = 970 \text{ M}_\odot \text{ yr}^{-1}$, assuming the radio/FIR relation $q = \log(\text{FIR}/3.75 \times 10^{12} \text{ Hz})/S_{1.4 \text{ GHz}}$ (Helou et al. 1985), with $q = 2.34$ (Yun et al. 2001), a correction factor of 2.3 to total IR luminosity (TIR) appropriate for hotter dust SEDs (Dale & Helou 2002), and the conversion from Kennicutt (1998)

$$\text{SFR}(\text{M}_\odot \text{ yr}^{-1}) = 1.8 \times 10^{-10} L_{8-1000 \mu\text{m}}(L_\odot).$$

The SFRs from their dust-corrected rest-frame 1500 \AA continuum flux are factors $\sim 50\times$ less (as described in C04), and the UV emission is clearly not probing the true luminosities of these systems (Table 3). The $\text{H}\alpha$ emission line suggests SFRs (Table 3) ten times less than the radio ($\langle \text{SFR}_{\text{H}\alpha} \rangle = 92$), although with the average extinction factor of $A_V \sim 2.9 \pm 0.5$ proposed for SMGs in Takata et al. (2006), this becomes $\langle \text{SFR}_{\text{H}\alpha, \text{corr}} \rangle = 1300 \text{ M}_\odot \text{ yr}^{-1}$. This is consistent, on average, with the radio-inferred SFRs, although the individual radio/ $\text{H}\alpha_{\text{corr}}$ ratios show very poor correspondence. We have, of course, argued in the case of RG J163655 that the CO(3–2) and the $\text{H}\alpha$ line emission may be coming from distinct regions, so these arguments do not obviously apply in every case, and the average correction factor applied to the $L_{\text{H}\alpha}$ may not be appropriate either individually or for the population. The $24\text{-}\mu\text{m}$ fluxes (Table 2) would represent strong supporting evidence for large SFRs. We calculate $\text{SFR}_{24\mu\text{m}}$ as in Pope et al. (2006) for consistency with SMGs (although strong $24\text{-}\mu\text{m}$ luminosities could also reveal a dominant hot AGN dust torus). In a large sample of SFRGs, the $24\text{-}\mu\text{m}$ luminosity distribution is indistinguishable from that of SMGs (Casey et al., 2008b). Two of our present three SFRGs have $24\text{-}\mu\text{m}$ observations, and only one is detected, the limit in the second case not being particularly constraining relative to the radio. The $\text{SFR}_{24\mu\text{m}}$ (Table 3) could be consistent with the $\text{SFR}_{\text{radio}}$ given uncertainties in calibrating the SFR indicators.

For a reference point – which can be scaled through by uncertainties in the SFR – we adopt the $\text{SFR}_{\text{radio}}$ and calculate surface densities Σ_{SFR} , and star-formation efficiencies ($\text{SFE} = L_{\text{FIR}}/M_{\text{H}_2}$) for the SFRGs, using assumed sizes described previously, and listed in Table 3. We find large SFEs ($4\times$ larger than the SMGs on average), although the observational constraints on the SFRs for the SFRGs are consistent with having been over-estimated by a factor $\sim 2 - 3\times$ which would bring them into reasonable agreement with the envelope of star-formation efficiencies for SMGs, LBGs and local ULIRGs.

We can also roughly estimate a lower limit to the gas to dust mass ratio where CO is detected (Table 3). We estimate similar dust mass limits for the SFRGs using

$$M_{\text{dust}}[M_\odot] = \frac{1}{1+z} \frac{S_{\text{obs}} D_L^2}{\kappa_d B(\nu_0, T_d)}$$

assuming $\kappa_\nu \propto \nu^\beta$, $\beta = +1.5$, and $B_\nu(T_d) \sim \nu^{+2}$ in the $M_{\text{dust}} < 1.6 \times 10^8 \text{ M}_\odot$ from the 2σ limit on the $850 \mu\text{m}$ flux of $\sim 2.2 \text{ mJy}$, assuming a dust mass absorption coefficient of $\kappa_{850\mu\text{m}} = 0.15 \text{ m}^2 \text{ kg}^{-1}$. We find ratios of 50 and 100, with at least a factor of ~ 6 uncertainty accounting for our uncertainty of the dust temperature ($\Delta T_d \simeq \pm 5 \text{ K}$), dust emissivity coefficient ($\Delta \beta \simeq \pm 0.5$), and mass absorption coefficient (about a factor of ~ 3 ; e.g. Seaquist et al. 2004).

Assuming the molecular gas reservoirs we detect are fueling the star formation within these galaxies, then there is enough gas to sustain the current star formation for $\tau_{\text{depletion}} \sim M(\text{H}_2)/\text{SFR}$ ranging from less than 9 to 13 Myr. Since we have also estimated stellar masses, we can compare the gas depletion time with the time to form the current stellar mass of the system. At the current SFRs, $\tau_{\text{formation}} \sim M_{\text{stars}}/\text{SFR}$ ranges from 80–240 Myr, which are comparable to the assumed ages of the stellar populations.

4.2. Comparison to other populations

Comparison of the SFRGs to the SMGs is of primary importance, since a major goal of the observations is to understand the degree to which SFRGs should be treated on a similar footing to SMGs in models and evolutionary calculations. Taking the average CO line luminosity and gas mass we find intrinsic line luminosities a factor of ~ 4 lower than the median for SMGs (cf. $\langle L'_{\text{CO}} \rangle = (3.8 \pm 2.3) \times 10^{10} L_\odot$ and $\langle M_{\text{gas}} \rangle = (3.0 \pm 1.6) \times 10^{10} \text{ M}_\odot$; Greve et al. 2005). The CO line width of RG J163655 is also much lower than the median of SMGs ($\langle \text{FWHM} \rangle = 780 \text{ km s}^{-1}$, Greve et al. 2005). Given the CO-inferred gas masses are somewhat low compared to SMGs we find, not surprisingly, that the gas depletion timescales are short compared to SMGs (which have $\tau_{\text{depletion}} \sim 40 \text{ Myr}$, Greve et al. 2005), though the SFRGs are still within a physically plausible range. We only have a useful constraint on the size of the emitting region for RG J123711 to compare with higher resolution images of SMGs, although in general the SFRGs exhibit similar radio sizes and morphologies to SMGs (compare Chapman et al. 2004b and Biggs & Ivison 2008 to Casey et al. 2008b). The typical gas to dynamical mass fraction in SMGs is estimated to be ~ 0.3 assuming a merger model (Greve et al. 2005), while they have SFEs

TABLE 1
PROPERTIES OF CO OBSERVED SFRGs

RA	Dec	z(CO)	z(UV)	z(H α)	L _{FIR,radio} 10 ¹² L _⊙	T _d K	S _{CO} Jy km s ⁻¹	L' _{CO} 10 ¹⁰ K km s ⁻¹ pc ²	FWHM _{CO} km s ⁻¹	M _{dyn} 10 ¹⁰ M _⊙	M _{gas} 10 ⁹ M _⊙
16 36 55.04	41 04 32.0	2.189	2.186	2.192	7.1±0.9	> 46	0.34 ± 0.07	1.04±0.21	410±40	8.4 sin ² i	8.3±1.7
13 12 36.01	42 40 44.1	...	2.240	2.243	6.7±0.6	> 48	< 0.27 ^a	< 0.71	< 5.6
12 37 11.34	62 32 31.0	~1.996	...	1.996	16.7±0.7	> 45	0.70 ± 0.22	1.93±0.60	15.4±4.8

a) For RG J131236, we set a limit for a 500 km s⁻¹ FWHM line centered at the H α redshift.

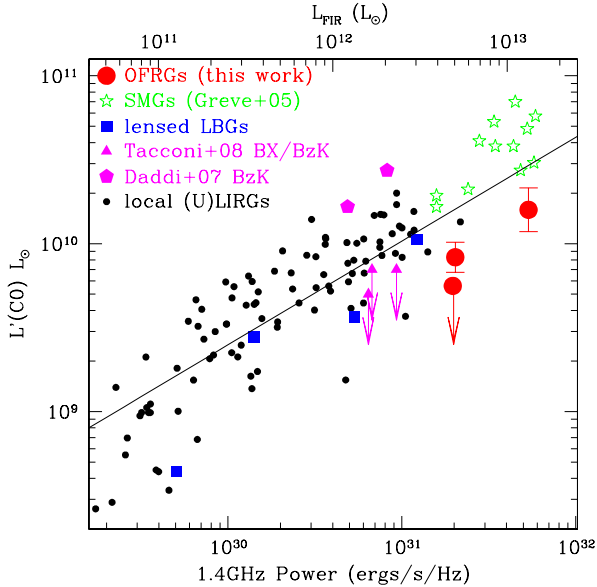


FIG. 3.— A comparison of the CO and radio luminosities for the three SFRGs described here, the SMGs from Greve et al. (2005) and Tacconi et al. (2006), the lensed LBGs detected in CO (Baker et al. 2004, Coppin et al. 2007, Kneib et al. 2005), the luminous $z \sim 2$ BX/BzK galaxies undetected in CO (Tacconi et al. 2008) and the two $z \sim 1.4$ BzK galaxies detected in CO by Daddi et al. (2008). The solid line is the best-fitting relation with a form of $\log L'_{\text{CO}} = \alpha \log L_{\text{FIR}} + \beta$ to the local LIRGs and ULIRGs and the high-redshift SMGs from Greve et al. (2005) (however it is no longer quite the best fit when radio luminosity is considered consistently across the populations). With gas conversions fixed, the SFRGs appear to have lower CO gas masses than SMGs, although if the radio-inferred SFRs are overestimated then the SFRGs could still lie on the plotted gas/SFR relation.

of $L_{\text{FIR}}/M_{\text{H}_2} \sim 450 \pm 170 \text{ L}_{\odot} \text{ M}_{\odot}^{-1}$ (Greve et al. 2005), gas-to-dust mass ratios of ~ 200 (with a factor of a few uncertainty in the dust mass alone) and gas surface densities of $\sigma_{\text{gas}} \sim 3000 \text{ M}_{\odot} \text{ yr}^{-1} \text{ pc}^2$ (Tacconi et al. 2006). Borys et al. (2005) estimate the average stellar mass for SMGs at $z > 1.5$ to be $3.2^{+3.4}_{-1.6} \times 10^{11} \text{ M}_{\odot}$, slightly larger than the average $1.8 \times 10^{11} \text{ M}_{\odot}$ for our three SFRGs.

Overall, this comparison suggests that SFRGs may be somewhat smaller mass objects (lower stellar mass, lower CO mass and lower dynamical mass) than SMGs, but share with them a large radio luminosity. The SFRs of both SMGs and SFRGs are subject to sizable uncertainties, not least of which is the initial mass function (e.g., Baugh et al. 2005). Pope et al. (2006) have pointed out that SMG SFRs estimated from the $24 \mu\text{m}$ *Spitzer*-MIPS observations are lower than those estimated from

the $850 \mu\text{m}$ or radio wavebands, although this could represent an issue of relative calibrations of these indicators in this luminosity regime rather than intrinsic properties.

We can also compare the SFRGs to local populations and less luminous star-forming galaxies at $z \sim 2$. Locally, L'_{CO} increases with L_{FIR} for (U)LIRGs, with the Greve et al. (2005) sample of SMGs extending this trend out to the highest far-IR luminosities ($\gtrsim 10^{13} \text{ L}_{\odot}$). For comparison, in Fig. 3 we have plotted the SFRGs on the $L'_{\text{CO}}-L_{\text{FIR}}$ diagram along with SMGs lying on the local relation, as well as three LBGs from the literature within the considerable uncertainties in their far-IR luminosities, three undetected BX/BzK galaxies (Tacconi et al. 2008), and two CO-detected BzK galaxies (Daddi et al. 2008 – these sources lie above the relation). The SFRGs lie somewhat below this relation.

5. DISCUSSION

As our calculations above have shown, it is very difficult to estimate the precise gas masses for SFRGs due to various uncertainties. However, a potentially important result emerges from these CO observations: compared to SMGs, SFRGs appear to be significantly more efficient at producing stars from a given molecular gas mass. If this is strictly true, then SFRGs cannot be interpreted as *scaled up* versions of local ULIRGs as Tacconi et al. (2006, 2008) have argued is the case for SMGs, since their gas masses appear to be lower than expected for their radio luminosities. There are two considerations to be taken into account here. Firstly, the far-IR luminosities and thus SFRs may be over-estimated from the radio, for instance if buried AGN were present. While none of these sources have AGN signatures in their UV or optical spectra, a deeply obscured AGN could still be driving a significant portion of the radio luminosity (e.g., Daddi et al. 2007b; Casey et al. 2008a). A further possible complication comes again from the radio selection of these objects. There is a ~ 0.25 dex scatter in the radio-FIR relation (Yun et al. 2001), and while locally there is no apparent correlation between SED shape and radio-FIR scaling, it is possible in our SFRGs that we are selecting galaxies which are amongst the lower 0.25 dex (weaker FIR per unit radio). If the SFRs in our galaxies were several times lower then the efficiencies would be similar to the average SMG (Fig. 3). Secondly, the conversion from CO(3–2) to molecular gas mass may not be the same as for SMGs. If α_{CO} were greater than the ~ 1 estimated for local ULIRGs (and as inferred to be correct for SMGs), these SFRGs could make up the shortfall in molecular gas mass from the average SMG ($\sim 4\times$), although the conversion would have to approach that typically adopted for the Milky Way $\alpha_{\text{CO}} = 4.6$ (Solomon & van den Bout

TABLE 2
PHOTOMETRIC PROPERTIES OF SFRGs

source	20cm μJy	850 μm mJy	350 μm mJy	24 μm μJy	8.0 μm μJy	5.8 μm μJy	4.5 μm μJy	3.6 μm μJy	I AB mag	R AB mag
RG J163655	43.9 \pm 7.1	-1.5 \pm 1.1	13.7 \pm 6.9	< 150	14.4 \pm 2.7	16.8 \pm 3.5	11.9 \pm 1.1	9.9 \pm 0.7	23.5	23.8
RG J131236	48.7 \pm 4.1	0.4 \pm 1.1	8.4 \pm 2.7	< 11	7.0 \pm 1.1	5.4 \pm 0.7	24.2	25.0
RG J123711	133.1 \pm 5.1	2.2 \pm 1.2	...	531 \pm 8	37.5 \pm 0.8	42.1 \pm 1.2	35.8 \pm 0.3	32.3 \pm 0.2	24.9	25.8

TABLE 3
DERIVED PROPERTIES OF THE SFRGs

source	SFR _{radio} $\text{M}_\odot \text{ yr}^{-1}$	SFR _{UV} $\text{M}_\odot \text{ yr}^{-1}$	SFR _{Hα} $\text{M}_\odot \text{ yr}^{-1}$	SFR _{24μm} ^a $\text{M}_\odot \text{ yr}^{-1}$	SFE ^b $\text{L}_\odot/\text{M}_\odot$	Σ_{gas} $\text{M}_\odot \text{ yr}^{-1} \text{ kpc}^{-2}$	M* ^c M_\odot	gas/dust ^d	$\tau_{\text{depletion}}$ (Myr)	$\tau_{\text{gas to stars}}$ (Myr)
RG J163655	630 \pm 120	46 \pm 11	150 \pm 50	< 255	600	70	1 \times 10 ¹¹	52	13.2	160
RG J131236	610 \pm 91	33 \pm 16	110 \pm 40	–	< 1450	< 65	5 \times 10 ¹⁰	–	< 9.2	80
RG J123711	1670 \pm 113	11 \pm 10	16 \pm 9	880 \pm 54	1330	35	4 \times 10 ¹¹	100	9.2	240

a) SFR from 24 μm luminosity, assuming the average SED in Dale & Helou (2002).

b) Star formation efficiency (SFE) is the SFR divided by the molecular gas mass.

c) Stellar mass calculated as Borys et al. (2005), adopting their $\text{L}_K/\text{M}_\odot = 3.2$.

d) No limit is possible for RG J131236 since both gas and dust are limits.

2005). This is unlikely given that the SFRGs often show clear evidence in high-resolution radio observations for merger-driven starbursts (Casey et al. 2008b).

It is noteworthy that while our observations have highlighted an ultraluminous $z \sim 2$ population which may build stars in an extremely efficient mode (or at least as efficient as SMGs if their SFRs are overestimated by factors of several), recent observations (Daddi et al. 2008) have identified a population of $z \sim 1.5$ galaxies which they detect in CO(2–1) exhibiting the opposite property: low-efficiency star formation. These Daddi et al. galaxies are selected as large massive disk-like galaxies, and it is perhaps not surprising that they form stars in an apparently quiescent “spiral-galaxy” mode. Nonetheless, it is intriguing that galaxies in the high-redshift Universe have been discovered with such a wide range of star-forming efficiencies (from poor to extreme) all lying in the $10^{12-13} \text{ L}_\odot$ regime. Massive galaxies are being built in a variety of modes in the $z = 1-3$ peak star-formation period.

The short depletion times compared to the long times to form the stellar masses suggests we may be seeing SFRGs in the last phase of their current star-formation episodes. However, one would expect on average to find SFRGs as a population half-way through their gas consumption lifetimes. In this context, the small ages imply either a very high duty cycle or that the SFRs are over-estimated from the radio luminosity. We reiterate that the large FIR luminosity estimates for our SFRGs are based mainly on the radio/FIR relation which is apparently applies for SMGs (Kovacs et al. 2006), but is only marginally supported for SFRGs through the 24- μm luminosity and dust-corrected H α measurements. It is possible that we are over-estimating their star-formation activity, which would lead us to under-estimate the duration timescales above.

We also note that the observed CO may be closely associated with the star formation, and thus is probably warm and highly visible (i.e. with low α_{CO}). It does

not rule out the existence of a cooler less visible component (with high α_{CO}), not intimately associated with the current zone of star formation (e.g. in the inner disk), which may still become available within its own dynamical timescale to fuel star formation. The result above may therefore be affected by the selection for the highly visible component of the molecular gas. However, the cold gas would need to be fairly widely distributed (to ensure that it doesn’t violate the dynamical limits on the total gas+stellar mass in the central regions), yet it must also be able to flow into the central regions on a timescale of <100 Myrs (near the limit of the gas sound speed $\sim 100 \text{ km/s}$).

In order to evaluate the implications of these results for massive galaxy formation, we recall that these three galaxies have typical characteristics for the SFRG population at all wavelengths measured. Our results underline the major role of gas consumption over short timescales and with high efficiencies, characterizing rapid and strong merger-driven bursts as a major growth mode for both stellar mass and black holes in the distant Universe. Even if the SFRs in these SFRGs were over-estimated by a factor of a few, they would remain ULIRG-class galaxies. If we assume that $\sim 50\%$ of the submm-faint SFRGs at $z \sim 2$ are dominated by star formation at levels comparable to SMGs, we arrive at a density of $\sim 5 \times 10^{-6} \text{ Mpc}^{-3}$, similar to that observed for SMGs (Chapman et al. 2003). Together, the SMGs and SFRGs represent a volume density $10\times$ smaller than measured for galaxies inferred to be forming stars at low efficiencies by Daddi et al. (2007b) which have space densities of order of 10^{-4} Mpc^{-3} . With SFRs a few to $10\times$ larger in the SMGs and SFRGs, the net effect is roughly equal numbers of stars being formed in both high- and low-efficiency modes at $z \sim 2$.

Further study should ascertain whether other SFRGs follow a similar pattern to the galaxies studied in this paper. A substantial sample will allow the properties of the gas to dynamical mass ratio to be determined accu-

rately for the population, since we only currently have one well-detected line profile, and the dynamical mass determination is limited by the unknown inclination.

6. CONCLUSIONS

- We conclude that the radio luminosities of these SFRGs are higher for their overall mass (gas plus stellar) than for the SMGs (given that if the radio-SFRs are over-estimated for one class, they could well be for both).
- We note that SMGs in general, and also these SFRGs, are outliers of the stellar mass-SFR correlation (Daddi et al. 2007a), probably due to the higher efficiency in forming stars for a similar stellar mass and CO luminosity. Lower gas masses in the SFRGs would imply even higher SFEs than the SMGs. By contrast, if the SFRs are significantly over-estimated by the radio, or the CO-to-H₂ conversion were significantly different from SMGs, then SFRGs could have similar efficiencies to typical ULIRGs. Together with the apparent low-efficiency star-forming (U)LIRGs from Daddi et al. (2008), the SMGs and SFRGs with SFRs several to 10 \times larger than the Daddi et al. galaxies suggest roughly equal numbers of stars being formed in both high- and low-efficiency modes at $z \sim 2$. Massive galaxies are being built in an impressive variety of modes in the $z = 1-3$ peak star-formation period.
- If the radio-inferred SFRs are correct, then these SFRGs are more efficient star formers than SMGs, and

cannot obviously be interpreted as *scaled up* versions of local ULIRGs as Tacconi et al. (2006, 2008) have argued is the case for SMGs. The SFRGs' radio luminosities are larger than would naturally scale from local ULIRGs given the gas masses or gas fractions. These observed gas masses and star-formation properties may be typical of the SFRG population and further work is justified to explore this population with improved statistics.

- Our results underscore the fact that ultraluminous galaxies in the high-redshift Universe have been discovered with a wide range of star-forming efficiencies, the SFRGs apparently being one extreme. Massive galaxies are likely being built in a variety of modes in the $z = 1-3$ peak star-formation period.

ACKNOWLEDGEMENTS

We thank an anonymous referee for a very careful reading and helpful comments. This work is based on observations carried out with the IRAM Plateau de Bure Interferometer. IRAM is supported by INSU/CNRS (France), MPG (Germany) and IGN (Spain). SCC acknowledges a fellowship from the Canadian Space Agency and an NSERC discovery grant. IRS acknowledges support from the Royal Society. AMS acknowledges support from STFC. We acknowledge the use of GILDAS software (<http://www.iram.fr/IRAMFR/GILDAS>).

REFERENCES

- Barger, A., Cowie, L., & Richards, E., 2000, *AJ*, 119, 2092
 Baker, A.J., Tacconi, L.J., Genzel, R., Lehnert, D., & Lutz, D., 2004, *ApJ*, 604, 125
 Baugh, C.M., Lacey, C.G., Frenk, C.S., Granato, G.L., Silva, L., Bressan, Benson, A.J., & Cole, S., 2005, *MNRAS*, 356, 1191
 Biggs, A.D., Ivison, R.J., 2006, *MNRAS*, 371, 963
 Biggs, A.D., Ivison, R.J., 2008, *MNRAS*, 385, 893
 Blain, A.W., Smail, I., Ivison, R.J., Kneib, J.-P., & Frayer, D.T., 2002, *Phys. Rep.*, 369, 111
 Blain, A.W. 1999, *MNRAS*, 309, 955
 Borys, C., Chapman S.C., Halpern M., Scott D., 2003, *MNRAS*, 344, 385
 Borys, C., Smail, I., Chapman, S.C., Blain, A.W., Alexander, D.M., & Ivison, R.J., 2005, *ApJ*, 635, 853
 Calzetti, D., Armus, L., Bohlin, R.C., Kinney, A.L., Koornneef, J., & Storchi-Bergmann, T., 2000, *ApJ*, 533, 682
 Carilli, C.L., & Wang, R., 2006, *AJ*, 132, 2231
 Casey, C., et al. *MNRAS*, 2008, submitted
 Chapman, S.C., et al. 2000, *MNRAS*, 319, 318
 Chapman, S.C., Richards, E., Lewis, G., Wilson, G., & Barger, A., 2001, *ApJ*, 548, L147
 Chapman, S.C., Lewis, G., Scott, D., Borys, C., & Richards, E., 2002, *ApJ*, 570, 557
 Chapman S., Blain A., Ivison R., Smail I., 2003, *Nat*, 422, 695
 Chapman, S.C., Barger, A., Cowie, L., Scott, D., Borys, C., Lewis, G., Richards, E., Steffan, A., & Wilson, G., 2003, *ApJ*, 585, 57
 Chapman S.C., Smail I., Blain A., Ivison R., 2004, *ApJ*, 614, 671
 Chapman S.C., Smail, I., Windhorst, R., Muxlow, T., & Ivison, R.J., 2004, *ApJ*, 611, 732
 Chapman S.C., Blain A., Smail I., Ivison R., 2005, *ApJ*, 622, 772
 Daddi, E., et al. 2007a, *ApJ*, 670, 156
 Daddi, E., et al. 2007b, *ApJ*, 670, 173
 Daddi, E., et al. 2008, *ApJ*, 673, L21
 Dale, D.A., & Helou, G., 2002, *ApJ*, 576, 159
 Dale, D.A., Helou, G., Contursi, A., Silberman, N.A., & Kolhatkar, S., 2001, *ApJ*, 549, 215
 Desai, V., et al. 2006, *ApJ*, 641, 133
 Greve, T.R., et al. 2005, *MNRAS*, 359, 1165
 Hainline, L.J. et al. 2008, *ApJ*, in press
 Helou G., Soifer B., Rowan-Robinson, M., 1985, *ApJ*, 298, L7
 Hinshaw, G., et al., 2008, *arXiv0803.0732*
 Houck, J., et al. 2005, *ApJ*, 622, 105
 Hughes, D.H., et al. 1998, *Nat*, 394, 241
 Ivison, R.J., et al. 2002, *MNRAS*, 337, 1
 Ivison, R.J., et al. 2007a, *ApJ*, 660, L77
 Ivison, R.J., et al. 2007b, *MNRAS*, 380, 199
 Kennicutt, R.C., Jr., 1998, *ApJ*, 498, 541
 Kneib, J.-P., Neri, R., Smail, I., Blain, A., Sheth, K., van der Werf, P., & Knudsen, K.K., 2005, *A&A*, 434, 819
 Kovacs, A., Chapman, S.C., Dowell, C.D., Blain, A.W., Ivison, R.J., Smail, I., & Phillips, T.G., 2006, *ApJ*, 650, 592
 Leitherer, C., et al. 1999, *ApJS*, 123, 3
 Menendez-Delmestre, K., et al., 2007, *ApJ*, 655, 65
 Pope, A., et al. 2006, *MNRAS*, 370, 1185
 Pope, A., et al. 2008, in press
 Sajina, A. et al. 2007 (*astro-ph/0705.3377*)
 Scott, S.E., et al. 2002, *MNRAS*, 331, 817
 Seaquist E., Yao L., Dunne L., et al. 2004, *MNRAS*, 349, 1428
 Smail, I., Ivison, R.J., & Blain, A.W., 1997, *ApJ*, 490, L7
 Smail, I. et al. 2007, *ApJ*, 654, 33
 Solomon, P.M., & Vanden Bout, P.A., 2005, *ARA&A*, 43, 677
 Solomon, P.M., Downes, D., Radford, S.J.E., & Barrett, J.W., 1997, *ApJ*, 478, 144
 Spergel, D.N., et al. 2003, *ApJS*, 148, 175
 Steidel, C. C., Shapley, A. E., Pettini, M., Adelberger, K. L., Erb, D. K., Reddy, N. A., & Hunt, M. P. 2004, *ApJ*, 604, 534
 Swinbank, A.M., Smail, I., Chapman, S.C., Blain, A.W., Ivison, R.J., & Keel, W.C., 2004 *ApJ*, 617, 64
 Swinbank, A.M., Smail I., Bower R., Borys C., Chapman S., et al., 2005, *MNRAS*, 359, 401
 Swinbank, A.M., Chapman, S.C., Smail, I., Lindner, C., Borys, C., Blain, A.W., Ivison R.J., & Lewis, G.F., 2006, *MNRAS*, 371, 465
 Tacconi, L.J., et al. 2006, *ApJ*, 640, 228
 Tacconi, L.J., et al. 2008, *ApJ*, in press
 Valiante, E., et al., 2007, *ApJ*, 660, 1060
 Weedman, D., et al. 2006a, *ApJ*, 638, 613
 Weedman, D., et al. 2006b, *ApJ*, 651, 101
 Yan, et al. 2005, *ApJ*, 628, 604
 Yan, et al. 2007, *ApJ*, 658, 778
 Yao, L., Seaquist E.R., Kuno N., & Dunne L., 2003, *ApJ*, 588, 771
 Yun, M., Reddy, N., & Condon, J., 2001, *ApJ*, 554, 803